Geologic map of the Samaniego Hills, Pinal and Pima Counties, southern Arizona

by

Charles A. Ferguson[1], Wyatt G. Gilbert[1], Tim R. Orr[1], Jon E. Spencer[1], Stephen M. Richard[1], Philip A. Pearthree[1], and Lisa Peters[2]

Arizona Geological Survey
Open-File Report 99-17

August, 1999
Revised September, 2000

Arizona Geological Survey
416 W. Congress, Suite 100, Tucson, AZ 85701

Includes 17 page text, 1:24,000 scale geologic map (1 sheet)

Jointly funded by the Arizona Geological Survey and the United States Geological Survey STATEMAP Program, Contract # 98HQAG2064

---

[1] Arizona Geological Survey
[2] New Mexico Geochronological Research Laboratory, 801 Leroy Place, Socorro, NM 87801

Introduction

The Samaniego Hills are a low series of hills composed of flat-lying to gently-dipping early Miocene and possibly late Oligocene lava flows interbedded with thin units of volcaniclastic and locally non-volcaniclastic sandstone and conglomerate. The preserved sequence is approximately 600 meters thick. The top is not preserved, but the base is well exposed along the southern edge of the hills, where it overlaps K-feldspar porphyritic granite of probable Middle Proterozoic age invaded by diabase dikes. The diabase occurs as vertical and subhorizontal dikes, and is probably associated with the Middle Proterozoic Apache Group, which overlies the granite sparingly along the southern edge of the map area. The granitic rocks form a broad piedmont surface that grades up-slope to the southwest into the Silver Bell Mountains, which are dominated by Late Cretaceous volcanic, sedimentary, and hypabyssal plutonic rocks associated with the Silver Bell Caldera complex (Watson, 1964; Sawyer, 1996).

Previous Work

Eastwood (1970) investigated the volcanic stratigraphy, chemistry, petrology and geochronology of the Samaniego Hills, but did not produce a map of the area. Sawyer (1987) mapped a small area along the southwest edge of the hills, but the only pre-existing bedrock maps of the rest of the map area are the county maps of Wilson and Moore (1959) and Wilson and others (1960). Field and Pearthree (1993) describe the Quaternary geology of the area. Damon and Bickerman (1964), Shafiqullah, and others (1976), and Brooks and Snee (1996) dated volcanic rocks in the area.

Acknowledgments

Geologic mapping of the Samaniego Hills was funded by STATEMAP research grant #98HQAG2064 to the Arizona Geological Survey. We thank Dave Sawyer for helpful discussions, and Larry Fellows for consistent support of geologic mapping.

Methods

Bedrock geology of the Samaniego Hills was mapped during the winter and spring, 1999. Quaternary geology of the area was compiled from the work of Field and Pearthree (1993), and the unit symbols were changed slightly to reflect current usage. Quaternary geology of areas within Pima County were modified from Field and Pearthree (1993) using 1:24,000 scale, 1984, color air photos. Geology of the southernmost Samaniego Hills and the northeastern Silver Bell Mountains was compiled directly from Sawyer (1996) with minor changes to the Quaternary based on observation of the 1984 color air photos. The area mapped by Sawyer (1987; 1996) is shown for the sake of continuity and because this area includes a prominent structural feature of possible regional significance, the Ragged Top fault.

Tertiary Volcanic rocks; stratigraphy and age

Volcanic rocks of the Samaniego Hills range in composition from low-silica rhyolite to basalt (Eastwood, 1970). The volcanic stratigraphy of the area was deciphered by Eastwood (1970), and even though he did not make a map of the area, we found his

relative age designations and correlation of volcanic units to be very good. We add only two other volcanic units; a hornblende latite plug (Tlh) near the southern edge of the map area, and a crystal-poor andesite (Ta) along the southwestern edge of the map area.

The stratigraphic sequence dips gently to the north. The oldest widespread volcanic rock is a pyroxene trachyandesite (Tpt) that directly overlies basement and is overlain by a crystal-rich biotite trachyte (Ttb) in the south. These rocks are overlain by the basalt of Cerro Prieto (Tb), a distinctive, crystalline-matrix lava that occurs throughout the southern and central part of the range. The basalt of Cerro Prieto is overlain by the aphanitic trachyte of Sasco (Tsa) in the north. To the north of Sasco Road a different sequence of volcanic rocks is present, dominated by the trachyte of Sasco (Ts) which is divided into two subdivisions. Volcaniclastic and non-volcaniclastic sedimentary rocks are interbedded between most of the lava units throughout the range. Three separate map units are recognized; a basal sedimentary unit (Tso) composed of arkosic conglomerate and pebbly sandstone, and upper (Tcu) and lower (Tc) volcaniclastic conglomerate units which underlie and overlie the basalt of Cerro Prieto. The older of these (Tc) contains a mixture of local volcanic clasts as well as granite, and rare Cretaceous volcanic rocks and hypabyssal rocks of the Silver Bell Mountains. The age relationships of other volcanic units of limited extent are depicted on the stratigraphic correlation diagram of Sheet 1.

Lava units are differentiated principally by phenocryst assemblage. The flow textures and colors of the matrices of many of the lavas change dramatically over short distances within individual flows. There is some slight variability in the phenocryst assemblages of separate flows that are considered part of the same unit. Where appropriate, our unit descriptions include micropetrographic observations from Eastwood (1970) and our thin-sections. The sample numbers of thin-sections used to characterize the phenocryst assemblages are provided at the end of each description. We have adhered to Eastwood's (1970) nomenclature for naming the map units, but we have changed some names in accordance with the rules of stratigraphic nomenclature so that none of the units bear formal names. Petrographic names have also been changed based on where analyzed samples (Eastwood, 1970) plot on the chemical classification scheme of Le Bas and others (1986).

Available geochronology for rocks in the Samaniego Hills (Eastwood, 1970; Shafiqullah and others, 1976; Reynolds and others, 1986; Brooks and Snee, 1996) indicate an early Miocene age for the volcanic field with K/Ar whole rock and biotite ages ranging from about 23 to 16 Ma. The location of each age date is indicated on Sheet 1 and in Table 1. Some of Eastwood's (1970) conventional K/Ar ages are out of order in terms of known stratigraphic relationships, and all of the rocks that were dated at less than 20 Ma are fairly altered. Ages of about 26.6 Ma (Damon and Bickerman, 1964) for the rhyolite of Ragged Top and about 26 Ma (Banks and others, 1978) for the trachyte of Indian Head, a widespread lava unit in the Sawtooth Mountains (Ferguson and others, 1999) that is petrographically and geochemically similar to the trachyte of Sasco, indicate that the older parts of the volcanic field may be late Oligocene in age.

Regional correlations and structural significance

The chemistry and petrography of the volcanic rocks in the Samaniego Hills is very similar to the rocks in the nearby Sawtooth Mountains (Figure 1) with the Sawtooth Mountains being only slightly more felsic on average. The petrology of the volcanic rocks in the Sawtooth Mountains and Samaniego Hills is similar to those in the northerly adjacent Picacho Peak area. Alteration by K-metasomatism has severely changed the chemical composition of most of the rocks in the Picacho Peak area (Brooks, 1986), but has not affected volcanic rocks in the Samaniego Hills or Sawtooth Mountains. The petrography and the general stratigraphic sequence of crystal-poor mafic-intermediate lavas bracketing a sequence of crystal-rich dacitic to trachytic lavas is common to all three mountain ranges, and it is very likely that they represent a single, tectonically dismembered volcanic field (Figure 2). The greatest thickness of volcanic rock is preserved in the Picacho Peak area (between 1.5 and 2 km). Very coarse-grained granitic clasts are present throughout the Picacho Peak volcanic sequence suggesting a nearby source area composed of crystalline basement.

A subsurface bedrock ridge connects the Samaniego Hills and Picacho Mountains (Hardt and Cattany, 1965; Shafiqullah and others, 1976). Based on selected water-well driller's records (Hardt and others, 1965), the deepest sedimentary basin-fill over this arch is about 185 meters (600'). Structurally, the geology of the Samaniego Hills is very simple, but directly to the north, a similar sequence of lava in the Picacho Peak area is titled steeply to the northeast and cut by numerous moderately to gently southwest-dipping faults (Richard and others, 1999). Cross-section A-A' of sheet 1 connects with cross-section B-B' of Richard and others (1999). The nature of the structural transition between the two ranges is unknown, but is likely also marked by southwest-dipping normal faults that were active at the same time as the Picacho Mountains detachment fault, and probably related normal faults in the Picacho Peak area. Driller's records (Hardt and others, 1965) indicate that granite bedrock was penetrated directly below basin-fill at depths between 125 meters (400') and 185 meters (600') in most of the wells directly north of the Samaniego Hills. This suggests that a major southwest-side-down fault bounds the northeast flank of the Samaniego Hills.

The Ragged Top fault zone, a major, west-northwest-striking, steeply southwest-dipping, southwest-side-down fault with a large component of dextral offset separates the Samaniego Hills from the Silver Bell Mountains (Hagstrum and Sawyer, 1989; Sawyer, 1996). In the hangingwall of the Ragged Top fault zone, Cretaceous volcanic rocks are tilted east approximately 20-30 degrees and unconformably overlain by essentially flat-lying mid-Tertiary volcanic rocks that are probably correlative to the volcanic rocks of the Samaniego Hills. The Ragged Top fault zone is intruded by the 25.64 + 1.0 Ma (K/Ar biotite, Damon and Bickerman, 1964) rhyolite of Ragged Top which is in turn intruded by andesitic dikes that are probably correlative to flows in the Samaniego Hills. The youngest rock offset by the Ragged Top fault zone is an Upper Cretaceous granodiorite porphyry estimated at between 69-73 Ma (Hagstrum and Sawyer, 1989).

Because the Ragged Top fault zone is such an important feature relating to the geology of southern Arizona we dated sanidine phenocrysts from the rhyolite of Ragged Top using the $^{40}Ar/^{39}Ar$ single-crystal, laser fusion technique (Figure 3, Table 2, 3). The sample (F9-167) yields a gaussian distribution (Figure 3) if one 67.5 Ma xenocryst and

two crystals affected by an anomalous blank measurement are eliminated from the data set. The weighted mean age calculated from the twelve remaining crystals is 25.69 ± 0.06 Ma. The MSWD is outside the acceptable limit so the error has been adjusted. The xenocryst is probably derived from one of the Upper Cretaceous units in the Silver Bell Mountains. The age we determined is nearly identical to the K-Ar biotite 25.64 ± 1.0 Ma age of Damon and Bikerman (1964).

References

Banks, N. G., Dockter, R. D., Silberman, M. L., and Naeser, C. W., 1978, Radiometric ages of some Cretaceous and Tertiary volcanic and intrusive rocks in south-central Arizona: United States Geological Survey Journal of Research, v. 6, p. 439-445.

Brooks, W. E., 1986, Distribution of anomalously high K_2O volcanic rocks in Arizona: Metasomatism at the Picacho Peak detachment fault: Geology, v. 14, p. 339-342.

Brooks, W. E., and Snee, L. W., 1996, Timing and effect of detachment-related potassium metasomatism on $^{40}Ar/^{39}Ar$ ages from the Windous Butte Formation, Grant Range, Nevada: United States Geological Survey Bulletin 2154, 25 pp.

Damon, P. E., and Bickerman, M., 1964, Potassium-argon dating of post-Laramide plutonic and volcanic rocks within the Basin and Range province of southeastern Arizona and adjacent areas: Arizona Geological Society Digest, v. 7, p. 63-78.

Deino, A., and Potts, R., 1990. Single-Crystal $^{40}Ar/^{39}Ar$ dating of the Olorgesailie Formation, Southern Kenya Rift, J. Geophys. Res., 95, 8453-8470.

Eastwood, R. L., 1970, A geochemical-petrological study of mid-Tertiary volcanism in parts of Pima and Pinal Counties, Arizona: Tucson, University of Arizona, unpublished Ph.D. dissertation, 212 pp.

Field, J. J., and Pearthree, P. A, 1993, Surficial geologic maps of the northern Avra Valley-Desert Peak area, Pinal and Pima Counties, Southern Arizona: Arizona Geological Survey Open-file Report 93-13, 11 pp., 9 sheets, 1:24,000 scale.

Ferguson, C. A., Gilbert, W. G., Klawon, J. E., and Pearthree, P. A., 1999, Geologic map of the Sawtooth Mountains and the north end of the West Silver Bell Mountains, Pinal and Pima Counties, southern Arizona: Arizona Geological Survey Open-file Report 99-16, 25 pp., 1:24,000 scale map.

Hagstrum, J. T., and Sawyer, D. A., 1989. Late Cretaceous Paleomagnetism and clockwise rotation of the Silver Bell Mountains, South Central Arizona: Journal of Geophysical Research, v. 94, p. 17,847-17,860.

Hardt, W. F., and Cattany, R. E., 1965, Description and analysis of geohydrologic system in western Pinal County, Arizona: United States Geological Survey Open-file Report, Tucson, Arizona.

Hardt, W. F., and Cattany, R. E., and Kister, L. R., 1964, Basic Ground-Water data for western Pinal County, Arizona: Water Resources Report 18, Arizona State Land Department, prepared by the USGS, 59 pp., 1:328,800 scale map.

Le Bas, M. J., Le Maitre, R. W., Streckeisen, A., and Zanettin, B., 1986, A chemical classification of volcanic rocks based on the total alkali-silica diagram: Journal of Petrology, v. 27, p. 745-750.

Reynolds, S. J., Florence, F. P., Welty, J.W., Roddy, M. S., Currier, D. A., Anderson, A.V., and Keith, S. B., 1986, Compilation of Radiometric Age Determinations in Arizona, Arizona Geological Survey Bulletin 197, 258 p., 2 sheets, scale 1:1,000,000.

Richard, S. M., Spencer, J. E., Ferguson, C. A., and Pearthree, P. A, 1999, Geologic map of the Picacho Mountains and Picacho Peak, Pinal County, Arizona: Arizona Geological Survey Open-file Report 99-18, 43 pp., 2 1:24,000 scale sheets.

Samson, S.D., and, Alexander, E.C., Jr., 1987. Calibration of the interlaboratory $^{40}Ar/^{39}Ar$ dating standard, Mmhb-1, Chem. Geol., 66, 27-34.

Sawyer, D. A., 1987, Late Cretaceous caldera volcanism and porphyry copper mineralization at Silver Bell (unpublished Ph.D. dissertation): University of California at Santa Barbara, 400 pp.

Sawyer, D. A., 1996, Geologic map of the Silver Bell and West Silver Bell Mountains, southern Arizona: United States Geological Survey Open-file Report 96-006, 21 pp., 1 sheet, 1:48,000 scale.

Shafiqullah, M., Lynch, D. J., Damon, P. E., and Pierce, H. W., 1976, Geology, geochronology and geochemistry of the Picacho Peak area, Pinal County, Arizona *in* Wilt, J. C., and Jenney, J. P., (eds.), Tectonic Digest: Arizona Geological Society Digest 10, p. 305-324.

Steiger, R.H., and Jäger, E., 1977. Subcommission on geochronology: Convention on the use of decay constants in geo- and cosmochronology. Earth and Planet. Sci. Lett., 36, 359-362.

Taylor, J.R., 1982. An Introduction to Error Analysis: The Study of Uncertainties in Physical Measurements,. Univ. Sci. Books, Mill Valley, Calif., 270 p.

Wilson, E. D., and Moore, R. T., 1959, Geologic map of Pinal County, Arizona: Arizona Bureau of Mines, 1 sheet, scale 1:375,000 (now available as Arizona Geological Survey Map M-3-9).

Wilson, E. D, Moore, R. T., and O'Haire, R. T., 1960, Geologic map of Pima County, Arizona: Arizona Bureau of Mines, 1 sheet, scale 1:375,000 (now available as Arizona Geological Survey Map M-3-8).

Watson, B. N., 1964, Structure and petrology of the eastern portion of the Silver Bell Mountains, Pima County, Arizona (unpublished Ph.D. dissertation): University of Arizona, Tucson, 168 pp.

Table 1 Summary of geochronology data and location of samples for volcanic units of the Samaniego Hills. Older ages recalculated using new constants in Reynolds and others (1986). UTM (grid zone 12) locations (± 30 meters) based on lat-long information given in Reynolds and others (1986), written descriptions from individual reports, and adjustments required by location of map unit contacts on our map. The locations are accurate to within 30 meters in relation to the location on Sheet 1, but since these locations are interpretations they may not be very accurate in relation to the original sample location.

Sample number	map unit	age	technique	reference	UTM north	UTM east
RLE-20-68	Ts	15.63 ± 4.8 Ma	K/Ar whole rock	Eastwood, 1970	3601590	455025
RLE-27-67	Tb	18.05 ± 0.8 Ma	K/Ar whole rock	Eastwood, 1970	3597630	459250
RLE-27-68	Tpt	20.32 ± 1.2 Ma	K/Ar whole rock	Eastwood, 1970	3596030	458375
RLE-29-67	Tsa	21.17 ± 0.6 Ma	K/Ar whole rock	Eastwood, 1970	3598200	459820
UAKA 73-14	Ts	22.06 ± 0.45 Ma	K/Ar biotite	Shafiqullah and others, 1976	3601320	456825
RLE-31-68	Tb	22.15 ± 1.3 Ma	K/Ar whole rock	Eastwood, 1970	3592640	460835
PP-9	Ts	22.19 ± 0.12 Ma	$^{40}Ar/^{39}Ar$ biotite	Brooks and Snee, 1996	3601325	456450
RM-04-63*	Tr	25.64 ± 1.0 Ma	K/Ar biotite	Damon and Bickerman, 1964	3589525	453850
F9-167	Tr	25.69 + 0.06 Ma	$^{40}Ar/^{39}Ar$ sanidine	this report	3590305	454310

*sample located just to the south of the map area of Sheet 1

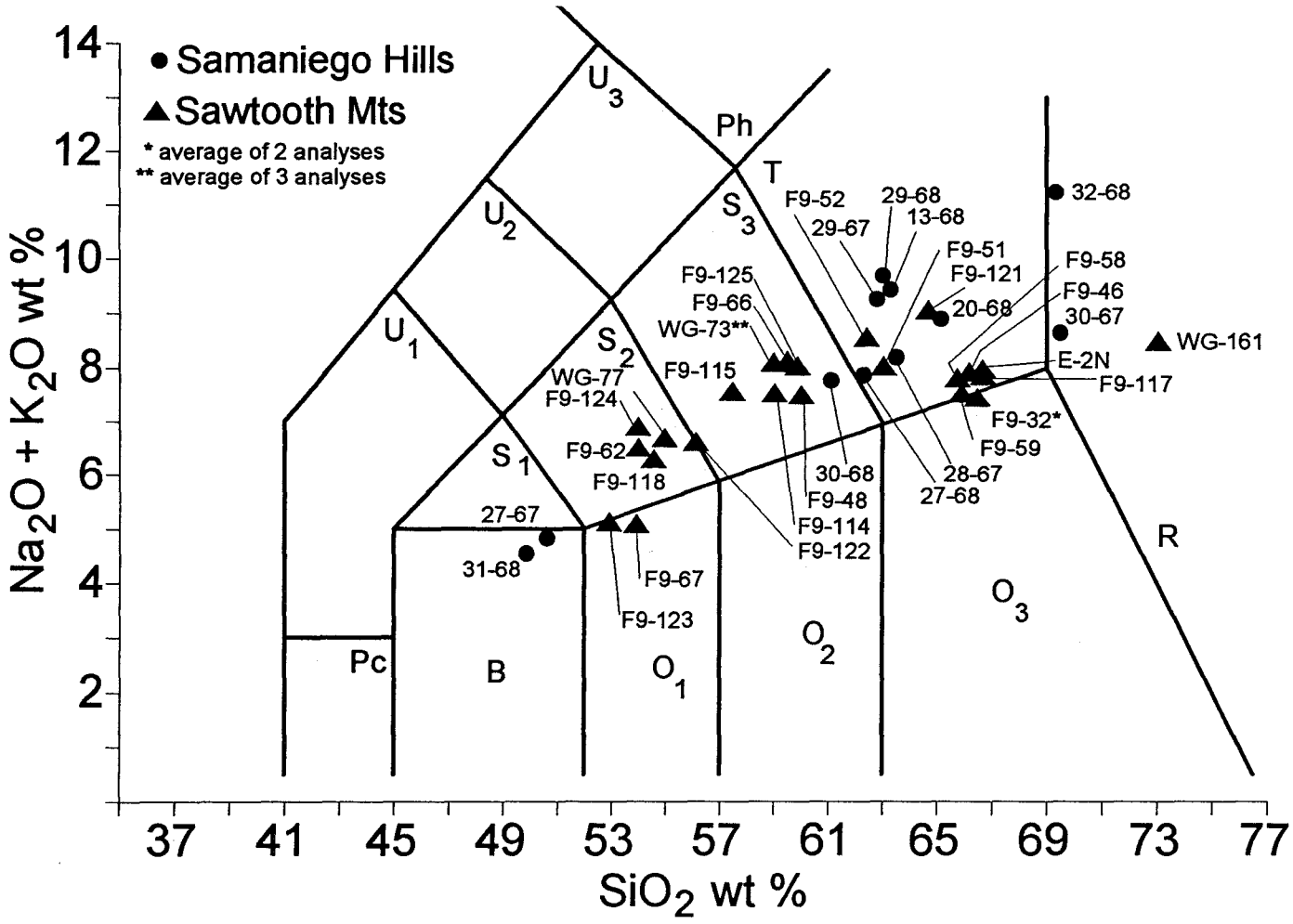

Figure 1 Total alkali versus silica diagram of Le Bas and others (1986) showing analyses from the Sawtooth Mountains (Ferguson and others, 1999), and analyses from the Samaniego Hills (Eastwood, 1970). Also shown is one analysis (E-2N) from an outlier of the trachyte of Indian Head (Sawtooth Mountains area) from Banks and others (1978). Field name abbreviations are Pc: picrobasalt, B: basalt, O_1: basaltic andesite, O_2: andesite, O_3: dacite, R: rhyolite, S_1: trachybasalt, S_2: basaltic trachyandesite, S_3: trachyandesite, T: trachyte, U_1: tephrite basalt, U_2: phonotephrite, U_3: tephriphonolite, Ph: phonolite.

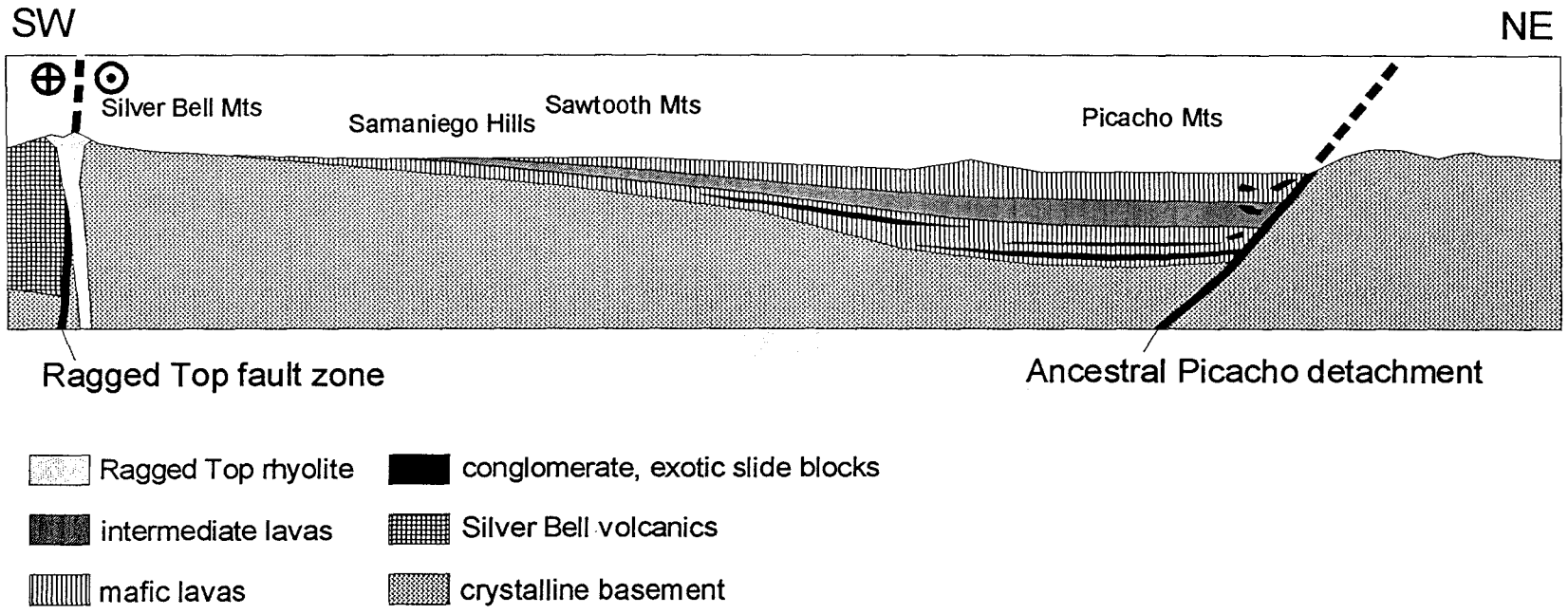

Figure 2 Hypothetical early Miocene structural cross-section of the composite Sawtooth Mountains - Samaniego Hills - Picacho Peak volcanic field and its relationship to two major faults. The northeastern basin-bounding normal fault probably evolved into the Picacho Mountains detachment. The Ragged Top fault is a major high-angle, dextral strike-slip, south-side-down structure along the south edge of the map area.

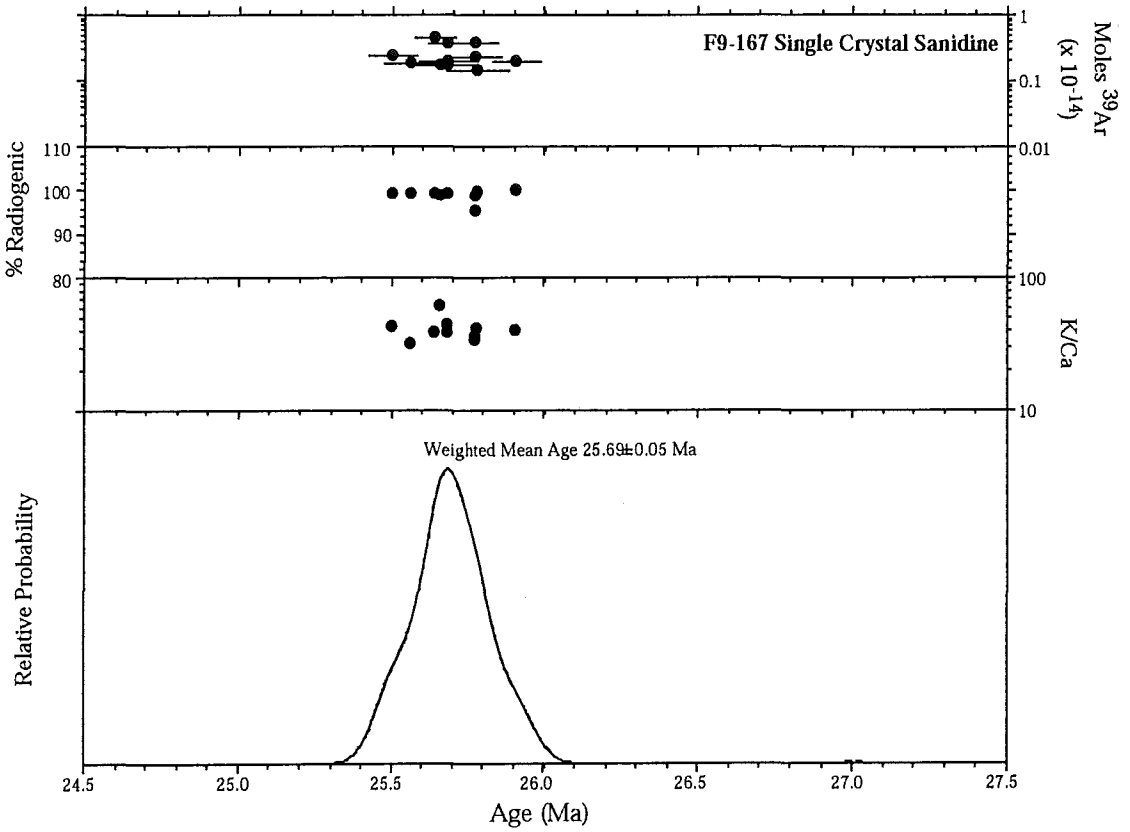

Figure 3 Age probability distribution diagram for sample F9-167.

Table 2 Analytical methods for the New Mexico Geochronological Research Laboratory

Sample preparation and irradiation:

Mineral phases concentrated by dissolving glass and matrix from the crushed rock in 15% HF. K-feldspar separated with standard heavy liquid, Franz Magnetic and hand-picking techniques.

K-feldspars were loaded into a machined Al disc and irradiated for 7 hours in D-3 position, Nuclear Science Center, College Station, TX.

Neutron flux monitor Fish Canyon Tuff sanidine (FC-1). Assigned age = 27.84 Ma (Deino and Potts, 1990) relative to Mmhb-1 at 520.4 Ma (Samson and Alexander, 1987).

Instrumentation:

Mass Analyzer Products 215-50 mass spectrometer on line with automated all-metal extraction system.

Single crystals were fused by a 10 watt Synrad CO2 laser.

Reactive gases removed during a 2 minute reaction with 2 SAES GP-50 getters, 1 operated at ~450°C and 1 at 20°C. Gas also exposed to a W filament operated at ~2000°C and a cold finger operated at -140°C.

Analytical parameters:

Electron multiplier sensitivity averaged 1.68 x 10-16 moles/pA.

Total system blank and background averaged 333, 10.0, 0.9, 1.8, 1.7 x 10-18 moles

J-factors determined to a precision of ± 0.1% by CO2 laser-fusion of 4 single crystals from each of 4 radial positions around the irradiation tray.

Correction factors for interfering nuclear reactions were determined using K-glass and CaF2 and are as follows: (40Ar/39Ar)K = 0.00020±0.0003; (36Ar/37Ar)Ca = 0.00028±0.000011; and (39Ar/37Ar)Ca = 0.00089±0.00003.

Age calculations:

Weighted mean age calculated by weighting each age analysis by the inverse of the variance.

Weighted mean error calculated using the method of (Taylor, 1982).

MSWD values calculated for n-1 degrees of freedom.

If the MSWD is outside the 95% confidence window (cf. Mahon, 1996; Table 1), the error is multiplied by the square root of the MSWD.

Decay constants and isotopic abundances following Steiger and Jäger (1977).

All final errors reported at ±2s, unless otherwise noted.

Table 3 Isotopic data for sample F9-167 from the rhyolite of Ragged Top.

ID	$^{40}Ar/^{39}Ar$	$^{37}Ar/^{39}Ar$	$^{36}Ar/^{39}Ar$ (x 10^{-3})	$^{39}Ar_K$ (x 10^{-15} mol)	K/Ca	$\%^{40}Ar^*$	Age (Ma)	±1σ (Ma)
F9-167, single crystal sanidine, J=0.0007640, NM-123, Lab#=51226								
08	18.75	0.0121	0.4054	2.31	42.0	99.4	25.50	0.06
03	18.83	0.0162	0.5420	1.83	31.4	99.2	25.56	0.07
07	18.89	0.0132	0.5345	4.54	38.6	99.2	25.64	0.05
15	18.95	0.0084	0.6952	1.68	60.6	98.9	25.66	0.08
06	18.89	0.0115	0.4192	1.65	44.5	99.3	25.68	0.07
04	18.86	0.0116	0.3336	1.89	44.0	99.5	25.68	0.08
14	18.93	0.0134	0.5488	3.77	38.0	99.1	25.69	0.05
05	19.73	0.0153	3.047	3.76	33.3	95.4	25.77	0.06
01	19.08	0.0139	0.8230	2.23	36.6	98.7	25.78	0.06
10	18.90	0.0124	0.2152	1.43	41.2	99.7	25.78	0.08
11	18.88	0.0127	-0.1718	1.88	40.3	100.3	25.91	0.06
02	18.17	4.748	-1.4397	0.073	0.11	104.5	26.09	1.13
12	*18.81*	*0.0142*	*-1.4365*	*0.646*	*36.0*	*102.3*	*26.33*	*0.13*
13	*18.99*	*0.0102*	*-1.7489*	*0.659*	*50.1*	*102.7*	*26.70*	*0.13*
09	*50.41*	*0.0151*	*1.610*	*1.09*	*33.8*	*99.1*	*67.55*	*0.16*
weighted mean		MSWD =2.9**	n=12		37.5	±13.9	25.69	0.05*

Notes:

n= number of analyses used for weighted mean calculation

Isotopic ratios corrected for blank, radioactive decay, and mass discrimination, not corrected for interferring reactions.

Individual analyses show analytical error only; weigthed mean age error includes error in J and irradiation parameters.

Analyses in italics are excluded from mean age calculations.

K/Ca = molar ratio calculated from reactor produced $^{39}Ar_K$ and $^{37}Ar_{Ca}$.

* 2σ error

** MSWD outside of 95% confidence interval

Unit Descriptions, Samaniego Hills

QUATERNARY

Unit descriptions and symbols modified slightly from Field and Pearthree (1993). 1993 unit symbols=new symbols: Y2r=Qycr, Y2rt=Qy2r, Y2=Qy2, Y1=Qy1, Y1p=Qy1p, Y=Qy, M2rt=Qlr, M2=Ql, M1=Qm.

Qycr **River channels and low terraces (< 0.1 ka)**: Active channels and floodplains of the larger drainages. Channels and overbank areas were not separately mapped because channel positions probably shift across these units fairly frequently. Deposits range from silt to coarse sands, but bars composed of well-rounded cobbles are common along the Santa Cruz River. The deposits are characterized by minimal soil development. Flooding occurs frequently in basin axis channels; larger floods inundate all **Qycr** outcrop areas.

Qy2r **Late Holocene river terraces (< 3 ka)**: Low terraces adjacent to active channels. Associated deposits are typically fine silt and sand with common gravel lenses of well rounded cobbles. Terrace surfaces are smooth and up to 4 m above the active basin axis drainages (**Qycr**). Some of these terraces were probably formed during historical arroyo cutting along the Santa Cruz River. Soil great group is Torrifluvents. Flooding occurs over large portions of these terraces during larger events.

Qy2 **Late Holocene alluvial fans, stream channels, and low terraces (estimated age < 4 ka)**: Late Holocene deposits comprise extensive alluvial fans in lower piedmont areas and restricted channel and low terrace deposits extending into upper piedmont areas and mountain ranges. Young alluvial fan deposits on the lower piedmont are composed of fine sand and silt. Active channels farther up-slope are composed of sand, silt, and gravel, generally coarsening closer to the mountains. Young alluvial fan surfaces are typically undissected and display distributary drainage patterns, although 1.5-m-deep arroyo cuts occur locally. Surfaces are typically smooth with very little bar and swale topography developed due to the fine-textured sediments. Desert pavement and rock varnish are absent. Minimal to no soil development has occurred. Typical soil great groups are Torrifluvents and Camborthids. These areas are subject to frequent to rare flooding.

Qy1 **Middle to early Holocene alluvial fans (estimated age 4 to 10 ka)**: Middle to early Holocene deposits primarily consist of extensive alluvial fans in middle piedmont areas and restricted terrace deposits in upper piedmont areas. **Qy1** deposits are slightly gravelly silty sand. Surface relief is typically less than 0.5 m above active channels. The surfaces are smooth and flat with an incipient dendritic drainage pattern. Weakly developed pebble to granule desert pavement is present over most of the surface. Desert varnish is absent. Minimal soil development has occurred in the underlying deposits. Soil great groups are Camborthids and

Torriorthents. These areas are not subject to frequent flooding. However, they should be regarded as potentially flood prone because they may be subject to flooding in extreme events and they could become subject to frequent flooding through aggradation of the shallow channels dissecting the surface.

Qy1p **Late to early Holocene pediment fans (estimated age 0 to 10 ka)**: Thin Holocene deposits covering pediment surface eroded into granite at the north end of the Silver Bell Mountains. Surface age is based on the minimal degree of soil development in the thin veneer of transported pebbly sand derived from weathering of the granite. Surface age should not be considered as the time of major pedimentation. Surface relief is typically less than 0.5 m above active channel bottoms. The pediment-fan surface is smooth and largely undissected, with small bedrock knobs protruding 5 to 20 m above the surface. Although shallow channels are present on the surface, no integrated drainage pattern is discernible on aerial photographs. Soil great groups are Camborthids and Torriorthents. These areas may be subject to occasional flooding.

Qy **Undifferentiated Holocene piedmont alluvial surfaces (estimated age 0 to 10 ka)**: In some places this designation is used where the **Qy1** and **Qy2** surfaces are too intricately intermingled to map separately at this scale. In some lower piedmont areas the designation is used where surface characteristics are not distinctive of either **Qy1** or **Qy2** surfaces but are clearly of Holocene age. These areas may be subject to rare to frequent flooding.

Qlr **Late Pleistocene river terraces (estimated age 10 to 150 ka)**: Relict terraces of the Santa Cruz River and Brawley Wash. These terraces are extensive in northern Avra Valley and between the Santa Cruz River and Interstate Highway 10. Deposits associated with these terraces are well-stratified sands and well-rounded gravels. The terrace surface is flat and is separated from the Qy2r terraces in places by a low scarp 0.5 to 3 m high. An incipient dendritic drainage pattern is developed on the surface with less than 0.5 m relief above channel bottoms except along the terrace scarp. Most of the surface is a grass covered plain, although portions are actively farmed. Silty sand covers the surface in most areas but an open granule to pebble desert pavement is locally present. A stage II to III calcic horizon is exposed in road cuts cut into the terrace. Soil great group is Haplargids. Stabilized eolian dunes of unknown age are locally present. **Qlr** surfaces generally are not prone to flooding. However, flooding has occurred locally on **Qlr** surfaces during historical times during extreme events and in areas of human disturbance.

Ql **Late Pleistocene alluvial fans and terraces (estimated age 10 to 150 ka)**: Late Pleistocene deposits consist primarily of extensive alluvial fans in middle piedmont areas, some restricted terraces inset into older deposits in lower piedmont areas, and a few small alluvial fans in upper piedmont areas. **Ql** deposits are a poorly sorted, angular to subangular admixture of silt, sand, and gravel. The surfaces are

moderately dissected with typically 1 to 3 m relief above active channels. Interfluve areas are broad and flat with a well-developed dendritic drainage pattern dissecting the surface. A poorly to moderately developed cobble to granule desert pavement is found over 50 to 80 percent of the surface. Surface cobbles are typically unvarnished although an orange color is sometimes seen on cobble undersides. Soil great groups are Camborthids and Haplargids. Most **Ql** areas are free from flooding, although those areas of low relief could become susceptible to flooding with relatively minor shifts in depositional patterns.

Qm **Middle to early Pleistocene alluvial fans (estimated age 150 to 1,000 ka)**: Deposits are a poorly sorted, angular to subangular admixture of silt, sand and gravel. The surfaces are moderately dissected with typically 1 to 6 m of relief above active channels but less than 2 m of relief above late Pleistocene (**Ql**) surfaces. Interfluve areas commonly are broad, flat, and smooth, but in areas of more intense erosion interfluves are rounded. A well-developed tightly interlocking cobble to pebble desert pavement is found in areas with volcanic gravels that have experienced little. Other areas exhibit an open cobble to granule pavement; sandy silt covers almost 50 percent of the surface. Volcanic cobbles are often varnished black (5YR 1.7/1) on top and reddish brown (2.5YR 4/8) on undersides. On felsic intrusive cobbles varnish is weakly developed to absent; the tops of cobbles are incompletely varnished black (7.5YR 2/1) while the undersides are brown (7.5YR 4/6). Underlying soils are characterized by moderately to very strongly developed argillic horizons (hue 5 to 2.5 YR), commonly overlying a stage IV calcic horizon. Soil great groups are Haplargids and Paleargids. These areas are isolated from active fluvial processes, and only entrenched channels are subject to flooding.

Qo **Early Pleistocene alluvial fans (estimated age > 1,000 ka)**: Volcanic boulder, cobble alluvium with abundant calcic crust debris in the soil. Surfaces are relatively flat and smooth and high-standing in relation to adjacent **Qm** fan surfaces.

MIOCENE

Sample number prefixes and corresponding investigators: RLE=Eastwood (1970), F9=Charles Ferguson, WG-Wyatt Gilbert, TO=Tim Orr, SR=Steve Richard, JS=Jon Spencer.

Tsu **upper flow unit of the trachyte of Sasco** See description below.

Ts **trachyte of Sasco** (formerly Sasco Andesite and Sasco flow-banded Andesite of Eastwood, 1970): Multiple flows displaying widely variable flow-textures comprise this unit, from streaky flow-banded, to massive or pervasively brecciated. The matrix is typically vitreous in appearance, and light or dark gray to black colored. Locally, alteration makes the rock appear dark red. The lavas are typically crystal-poor (3-7%), but locally, crystal-rich (25%) variations are present,

particularly in the vicinity of the Sasco smelter ruins where a vent complex for both crystal-poor and crystal-rich variations has been identified (Eastwood, 1970). The phenocryst assemblage is dominated by euhedral to subhedral, rounded plagioclase (0.5-2.0mm) An_{28-35}, and biotite (<3mm) with lesser amounts of rounded, embayed quartz (0.5-2.0mm), subhedral sanidine (0.5-1.0mm) in some instances rimmed by augite, augite, and rare hornblende. Microlites in the trachytic groundmass are predominantly plagioclase and pyroxene with variable amounts of biotite. Euhedral magnetite (0.05-0.1mm) is ubiquitous in all samples. Eastwood's (1970) chemical analyses (samples: 13-68, 20-68) show this rock to be a trachyte. Two variations of this unit have been described; an older brownish colored "flow-banded" unit (**Ts**) in the vicinity of Sasco, and a younger dark gray to light gray unit (**Tsu**) which makes up hills to the northwest. However, the two variations are essentially identical in terms of phenocryst assemblage, and there is apparently only one diagnostic micropetrographic feature that can be used to distinguish the two variations; the older unit contains spherical blebs of microdiorite < 5mm characterized by interlocking, needle shaped mafic minerals (0.5-1mm). The blebs are essentially impossible to identify in hand specimen. The intraformational contact shown in the W 1/2 sec. 18, T. 10 S., R. 9 E. separates the subdivisions. **Ts** micropetrographic samples: RLE-30-67, RLE-22-68, RLE-23-68, WG-48, WG-62a, WG-65, WG-66b, TO-23a. **Tsu** micropetrographic samples: RLE-13-68, RLE-14-68, RLE-20-68, RLE-21-68, WG-41, WG-45a. Other **Ts** samples: WG-46a,b, 47, 49a,b, 61, 62b, 63, 64a,b, 66a, TO-23b. Other **Tsu** samples: WG-44, 45b,c,d.

Tcu **upper conglomerate**: Coarse-grained volcaniclastic sedimentary rocks, locally including some probable volcanic breccia.

Tsab **brecciated aphanitic trachyte of Sasco**: Autobrecciated lava variant of the aphanitic trachyte of Sasco map unit. See below unit description.

Tsa **aphanitic trachyte of Sasco** (formerly Sasco aphanitic andesite of Eastwood, 1970): Light gray, vitreous-matrix trachyte containing less than 1% phenocrysts of rounded subhedral plagioclase (0.2-1.0mm), rare rounded quartz (0.2-1.0mm) commonly rimmed by augite, and lath-shaped hypersthene (≤2mm) also rimmed by augite. Chemical analyses show this rock to be a trachyte (Eastwood, 1970 samples: 28-67, 29-67). Micropetrographic samples: RLE-28-67, RLE-29-67, TO-16. Other samples: F9-55, TO-7,10,18, SR-2-9-99-1.

Tb **basalt of Cerro Prieto** (formerly Cerro Prieto Basalt of Eastwood, 1970): Crystalline matrix, gray basalt lava containing up to 10% clinopyroxene (pigeonite) and olivine (0.5mm) phenocrysts suspended in a highly crystalline matrix characterized by interlocking plagioclase crystals up to 3 mm long (An_{54-62}). The matrix texture is reminiscent of diabase, and non-vesicular, massive portions of the flows strikingly resemble this type of rock. The basalt occurs as amalgamated flows with little or no sedimentary interbeds. Chemical analyses show this rock

(Eastwood, 1970 samples: 27-67, 31-68) to be a true basalt. Micropetrographic samples: RLE-27-67, RLE-31-68, SR-2-11-99-1, SR-2-9-99-2,3, TO-25, JS-3-9-99-2. Other samples F9-53, 54, TO-20a,b, 25, JS-3-9-99-1, JS-3-11-99-3, 4.

Tc **conglomerate**: Medium- to thick-bedded sandstone, pebbly sandstone, and conglomerate containing clasts of basalt or pyroxene trachyandesite (70%), and dacite and granite (30%). The sand-sized fraction is typically arkosic. AZGS sample SR-2-10-99-5 was collected for potential detrital-grain geochronology.

Ta **pyroxene andesite** (new unit): Dark-colored, fine-grained, crystalline matrix andesitic lava, and hypabyssal rocks. Sample WG-192 contains 5-10% clinopyroxene (< 0.5mm), <1% orthopyroxene (0.5-1.0mm) in a crystalline matrix of plagioclase microlites. This unit is mapped only in the southwest in isolated outcrops, and its correlation or equivalence to rocks in the main part of the Samaniego Hills is unknown. Includes map units Ta and Tai of Sawyer (1996). Other samples: WG-108, F9-158, 159. The unit may correlate in part with the pyroxene trachyandesite (Tpt).

Ttb **biotite trachyte** (Eastwood, 1970): Crystal-rich lava containing up to 40% phenocrysts of plagioclase and orthoclase (0.1-1.0mm), biotite (0.1-1.5mm), and clinopyroxene (0.5-2.0mm) which commonly occurs in clumps with biotite and magnetite. A trace of orthopyroxene (1mm) rimmed by augite is also present, and some samples (SR-2-9-99-10) contain up to 2% hornblende (2-4mm). The matrix varies from crystalline to glassy, and in color from light gray to black or red. The unit includes coarse-grained monolithic breccia in the south and a series of dikes that were not mapped separately. Chemical analysis (Eastwood, 1970 sample 29-68) of this rock show it to be a trachyte. Micropetrographic samples: RLE-29-68, WG-191, SR-2-11-99-6, 7, SR-2-9-99-10, JS-2-18-99-3. Other samples: F9-70, WG-83, 106, SR-2-9-99-10, JS-2-18-99-4, 5, JS-3-9-99-3, 4, JS-3-11-99-2, 5.

Tbu **basalt undifferentiated**: Isolated exposures of basaltic lava with poorly constrained stratigraphic relationships to other volcanic rocks of the Samaniego Hills. The Tbu unit is overlain by three of the more widespread units in the western part of the map area: 1) the pyroxene andesite (Ta), 2) the biotite trachyte (Ttb), and 3) the upper flow unit of the trachyte of Sacso (Tsu). The unit is also interbedded with the upper conglomerate (Tcu). Phenocrysts in sample WG-42 comprise 5-10% plagioclase (0.5-4.0mm), 2% hornblende (0.5-1.0mm), 3-4% pyroxene (0.5-2mm), and a trace of biotite (0.5mm). Other samples: WG-43, F9-157, 160, 162.

Tlh **hornblende latite** (new unit): Dark gray to dark lavender lava and intrusive complex containing 10-15% euhedral, needle-shaped hornblende phenocrysts (1-4mm) and 3-4% pyroxene in a matrix of plagioclase microlites. Micropetrographic sample JS-2-18-99-2. Sample F9-77 is a potential geochronology specimen.

Tst **sandstone and tuff**: Thin- to medium-bedded volcaniclastic sandstone and/or non-welded tuff that is preserved at the base and around the periphery of a plug of the hornblende latite (Tlh) unit in the southern part of the map area. The unit also directly ovelies basement in this area, and it may also underlie the pyroxene trachyandesite (Tpt).

Tpt **pyroxene trachyandesite** (formerly pyroxene andesite of Eastwood, 1970): Lava containing up to 10% phenocrysts of euhedral hypersthene (0.2-2.0mm) $\pm$ olivine ($\leq$2mm), and rare plagioclase (<1mm). The unit occurs as amalgamated lava flows displaying widely variable textures and colors of matrix. The matrix ranges from glassy to finely crystalline and phenocryst content varies down to less than a few percent. The mafic phenocrysts are commonly very well preserved in the glassy matrix varieties. The average of two analyses (Eastwood, 1970 samples: 27-68, 30-68) show this rock to be a trachyandesite). Micropetrographic samples: RLE-27-68, RLE-30-68, SR-2-11-99-2, WG-109, WG-110, JS 3-11-99-1. Other samples: F9-68, 69, SR-2-9-99-6,7,8,9, SR-2-11-99-3,5, WG-82, 84, 85, 105, 107, 111, TO-28, 30, 31, 32, JS-2-18-99-1, JS-3-11-99-1.

Tr **rhyolite of Ragged Top** (Sawyer, 1996): Flow-banded intrusive rhyolite complex at Ragged Top. Lava and hypabyssal rocks contain 5-15% phenocrysts of orthoclase or sanidine and plagioclase (up to 5mm), and biotite (up to 3mm). Eastwood's (1970) chemical analysis of this rock (sample 32-68) shows it to be a low-silica rhyolite. Eastwood (1970) micropetrographic sample 32-68. AZGS geochronology sample F9-167.

Tso **older sedimentary rocks** (Sawyer, 1996): Medium- to thick-bedded arkosic sandstone and pebbly sandstone.

UPPER CRETACEOUS

Ksa **Andesite/dacite** (Sawyer, 1996): Lava flows and breccia of intermediate composition containing plagioclase, and lesser amounts of hornblende and biotite. Pyroxene phenocrysts are sparse to absent. Quartz phenocrysts characterize the dacitic varieties.

Kgp **Granodiorite porphyry** (Sawyer, 1996): Porphyritic hypabyssal rock containing 50%-80% phenocrysts of plagioclase and subordinate biotite, quartz, hornblende, and orthoclase.

Kcr **Caflin Ranch Formation** (Watson, 1964; Sawyer, 1996): Sedimentary rocks interpreted as moat-fill for the Silver Bell Caldera.

MIDDLE PROTEROZOIC

Yd **Diabase**: Medium to fine-grained diabase. Intrudes granite as dikes, and irregular-shaped bodies. AZGS sample: WG-81.

Ya **Apache Group undifferentiated** (Sawyer, 1996): Arkosic sandstone, conglomerate, and siltstone. Probably equivalent mostly to the Dripping Springs quartzite.

Yg **Granite**: Medium- to coarse-grained, K-feldspar porphyritic granite containing between 5-15% biotite. AZGS samples SR-2-11-99-4, JS-2-18-99-6, geochronology sample F9-166.